Acta Geodyn. Geomater.Vol.1, No.2 (134), 253-259, 2004

# REPRESENTATIVE STRUCTURES OF THE DUKLA COAL FROM UPPER SILESIAN COAL BASIN

**Pavel STRAKA [1]* and Helena ZUBKOVÁ [2]**

[1] *Institute of Rock Structure and Mechanics, Academy of Sciences of the Czech Republic, V Holešovičkách 41, CZ-182 09 Prague, Czech Republic*
[2] *Institute of Chemical Technology of Prague, Technická 5, CZ-162 08 Prague, Czech Republic*
**Corresponding author's e-mail:* straka@irsm.cas.cz

(*Received* June 2003, *accepted* October 2003)

ABSTRACT
$^{13}$C CP/MAS NMR structural parameters of the Dukla coal from Upper Silesian Coal Basin, Ostrava-Karviná District were determined. Aromatic-cyclanic structures were expressed and discussed. It was found that representative structures of the Dukla coal are the clusters with mainly with 1 – 2 aromatic rings, 1 OH groups and five- or six-membered cyclanes with methyls and quaternary carbons. As basic structures of bituminous coals from Upper Silesian Coal Basin are the clusters with mainly 3 – 4 aromatic rings, the clusters with mainly with 1 – 2 aromatic rings exist in the Dukla coal polymers as prevailing form of aromatic-cyclanic basic units.

KEYWORDS: coal, $^{13}$C CP/MAS NMR, coal structures

## INTRODUCTION

Chemical structure of most exploited bituminous coals from Upper Silesian Coal Basin has highly aromatic character. Upper Silesian coals contain three-, four- and five-rings clusters with four to six substituents. Almost higher is a part of ethereal oxygen comparing it with the hydroxyl ones and in the meantime the contents of ethereal and hydroxyl oxygen is much higher than the content of carbonyl oxygen. Also similar or mostly double portion of pyrrole nitrogen comparing it with pyridine ones is present; protonized form of pyridine nitrogen (pyridinium) and also its oxidized form (pyridine-N-oxide) are in minority. The proportion of thiophenic/aromatic sulfur compared with the aliphatic sulfur show that the thiophenic one dominate. The proportion of aromatically bound carbons is round 65 – 80 % of the content of carbons. But some coals from Upper Silesian Coal Basin (example coal from mine Dukla, Ostrava-Karviná District) have lower content of aromatic carbons and higher portion of aliphatic and cyclanic carbons. As maceral fractions of Upper Silesian coals have usually aromaticity 0.65 – 0.81, fractions of the Dukla coal have a lower aromaticity (0.63 – 0.65) and a significantly lower amount of aromatic bridgehead carbons in comparison with the other coals.

The aim of this work is to determine $^{13}$C CP/MAS NMR structural parameters of the maceral fractions of the Dukla coal by the use of combination of dipolar-dephasing with the CP/MAS integration techniques, to express representative aromatic-cyclanic structures of this coal and discusse the chemical structures of bituminous coal with lower aromaticity.

## EXPERIMENTAL

As samples, the solid separates obtained from bituminous coal Dukla from Upper Silesian Coal Basin – Ostrava-Karviná District were used. Powdered low-sulfur coal (Table 1) was mixed with xylene/tetrachloromethane solutions (densities of 1.21 – 1.50 g.cm$^{-3}$) and separated into parts with different apparent densities (Table 2) by sink float method and centrifugation (IFB 303X Alfa Laval centrifuge). Proximate, ultimate and petrographic analyses of separates obtained are presented in Tables 2 and 3.

**Table 1** Proximate, ultimate and petrographic analyses of coals used. $W^a$ – water content, $A^d$ – ash content (dry basis), $V^{daf}$ – volatile matter (dry ash free basis), $S^d_t$ – total sulfur (dry basis); H, C, $S_o$, N a O($^{daf}$) – ultimate analysis of coal substance (wt.-%); V, L, and I – contents in vitrinite, liptinite and inertinite (vol.-%), respectively

| Coal | $W^a$ | $A^d$ | $S^d_t$ | $V^{daf}$ | $H^{daf}$ | $C^{daf}$ | $S^{daf}_o$ | $N^{daf}$ | $O^{daf}_{dif}$ | V | L | I |
|---|---|---|---|---|---|---|---|---|---|---|---|---|
| Dukla | 1.6 | 10 .2 | 0 .7 | 33 .1 | 5 .02 | 81 .60 | 0 .74 | 1 .32 | 11 .33 | 63 | 15 | 22 |

**Table 2** Proximate and ultimate analyses of the coal separates obtained. ρ – apparent density of the separate. For other symbols see Table 1

| Sample | ρ | $W^a$ | $A^d$ | $V^{daf}$ | $C^{daf}$ | $H^{daf}$ | $N^{daf}$ | $S^{daf}_o$ | $O^{daf}_{dif}$ |
|---|---|---|---|---|---|---|---|---|---|
| No. | ( g . cm$^{-3}$) | | (wt.-%) | | | | (wt.-%) | | |
| *1* | <1.21 | 3.60 | 4.70 | - | 82.48 | 5.46 | 1.41 | 0.64 | 10.01 |
| *2* | 1.24–1.27 | 3.68 | 8.60 | 35.57 | 82.04 | 5.53 | 1.31 | 0.65 | 10.47 |
| *3* | 1.27–1.33 | 2.02 | 2.39 | 33.26 | 82.81 | 5.03 | 1.53 | 0.65 | 9.99 |
| *4* | 1.33–1.40 | 1.79 | 8.54 | 32.42 | 83.03 | 5.01 | 1.31 | 0.69 | 9.95 |
| *5* | 1.40–1.50 | 1.64 | 17.64 | 31.92 | 82.84 | 4.89 | 1.09 | 0.69 | 10.49 |
| *6* | >1.50 | 1.10 | 35.39 | 44.46 | 71.83 | 4.18 | 0.99 | 0.78 | 22.22 |

**Table 3** Petrographic analysis of the coal separates obtained. V, L, and I – contents in the maceral groups of vitrinite, liptinite and inertinite, respectively

| Sample No. | ρ ( g . cm$^{-3}$) | V | L | I |
|---|---|---|---|---|
| | | | (vol.-%) | |
| *1* | <1.21 | 34.4 | 52.3 | 13.3 |
| *2* | 1.24–1.27 | 61.1 | 20.7 | 18.2 |
| *3* | 1.27–1.33 | 67.9 | 7.4 | 24.7 |
| *4* | 1.33–1.40 | 65.5 | 9.8 | 24.7 |
| *5* | 1.40–1.50 | 34.2 | 17.7 | 48.1 |
| *6* | >1.50 | 27.4 | 20.8 | 51.8 |

$^{13}$C CP/MAS NMR spectra of the samples were measured with the spectrometer Bruker DSX 200 in 7 mm $ZrO_2$ rotor at the frequencies of 50.33 MHz and 200.14 MHz ($^{13}$C and $^1$H, resp.). Number of data points was 0.5 K, magic angle spinning frequency 5.0 kHz, “strength” of $B_1$ field ($^1$H and $^{13}$C) was 50.0 kHz. The number of scans for the accumulation of $^{13}$C CP/MAS NMR spectra was 3600 – 7200, repetition delay 3 s and spin lock pulse 1 ms. During the detection a high power dipolar-decoupling was used to eliminate strong heteronuclear dipolar coupling. $^{13}$C scale was calibrated by external standard glycine ($\delta$ = 176.03 ppm – low field carbonyl signal). For $^1$H-$^{13}$C dipolar-dephasing experiments standard pulse sequence was used where cross-polarization period was followed after $\tau$ delay by two simultaneous $\pi$ pulses on both ($^{13}$C and $^1$H) channels. Data acquisition starts after second $\tau$ delay. $2\tau$ delay was incremented from 2 to 200 μs. 24 increments were performed to obtain dipolar-dephasing dependence. The number of scans amounted to 400.

## EVALUATION OF $^{13}$C CP/MAS NMR SPECTRA

In the $^{13}$C CP/MAS NMR spectra obtained (Fig. 1) two low intensive spinning side bands SSB-Ar and SSB-Al corresponding to central signals of aromatic and aliphatic/cyclanic structures, respectively, were observed. The content of carbonyls was very low, below 0.5 %. Fraction of aromatic carbons – aromaticity $f_a$ – was calculated from the integral intensity of signals ($I_i$) according to the equation

$$f_a = \frac{2I_{SSB-Ar} + I_{Ar} - I_{SSB-Al}}{I_{SSB-Ar} + I_{Ar} + I_{Al} + I_{SSB-Al}} \qquad (1)$$

We supposed the same intensity of ± 1 spinning side bands SSB-Ar and SSB-Al, although the right-hand side SSB-Ar and the left-hand side SSB-Al are overlapped by central signals of aliphatic/cyclanic and aromatics structure units, respectively.

The aromatic signal ($\delta$ = 90 – 170 ppm) can be divided into protonated $f_a^H$ and nonprotonated $f_a^N$

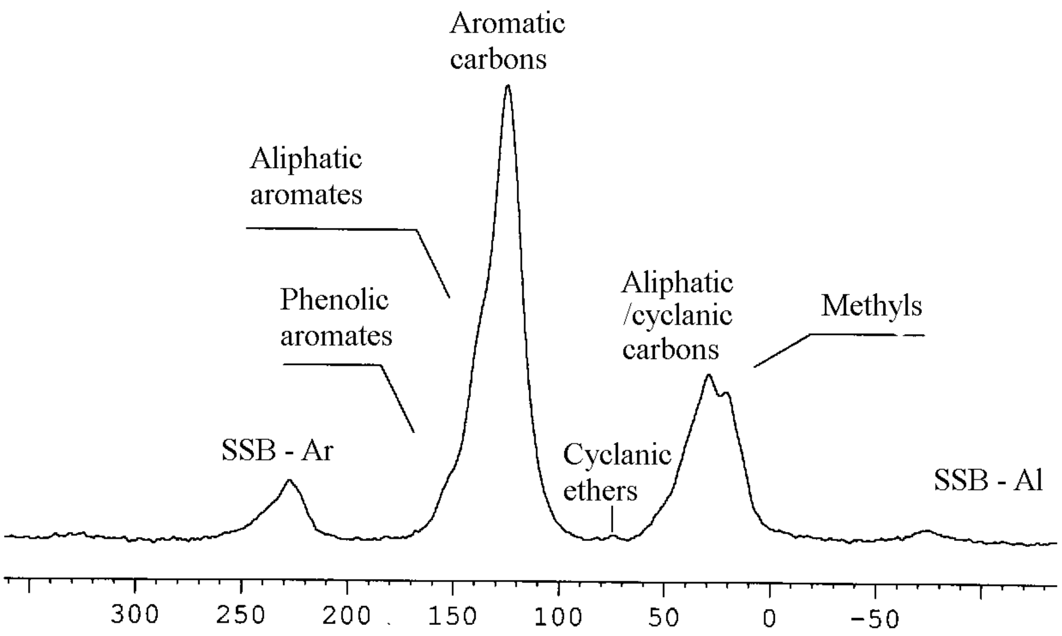

**Fig. 1** Typical $^{13}$C CP/MAS NMR spectrum of coal maceral fractions from the Dukla coal

carbon fractions according to a portion of Gaussian and Lorentzian magnetization decay measured by $^{1}$H-$^{13}$C dipolar-dephasing experiments (Solum, Pugmire and Grant, 1989):

$$f_a^H = f_a M_{0G} \tag{2}$$

$$f_a^N = f_a M_{0L} \tag{3}$$

$M_{0G}$ and $M_{0L}$ – initial magnetizations, Gaussian and Lorentzian, respectively – were calculated by fitting of experimentally determined dipolar-dephasing dependences according to the equation describing the decay of mixed Lorentzian and Gaussian carbon magnetization ($M$) through the Gaussian and Lorentzian dipolar-dephasing decay time constants $T_G$ and $T_L$, respectively:

$$M = M_{0L} \exp\left(-\frac{t}{T_L}\right) + M_{0G} \exp\left(-\frac{t}{T_G}\right) \tag{4}$$

The dipolar-dephasing decay time constants and the initial magnetizations are summarized for aromatic as well as aliphatic/cyclanic carbon signals in Table 4. Strongly coupled aromatic carbons with the Gaussian magnetization decay (protonated carbons) have decay time constants $T_G$ in a narrow range from 26 to 42 μs

**Table 4** Dipolar-dephasing decay time constants ($T_L$ – Lorentzian decay time constant, $T_G$ – Gaussian decay time constant,) and initial magnetizations ($M_{0L}$ – Lorentzian initial magnetization, $M_{0G}$ – Gaussian initial magnetization)

| Sample No. | Aromatic carbons | | | | Aliphatic/cyclanic carbons | | | |
|---|---|---|---|---|---|---|---|---|
| | $T_L$ (μs) | $T_G$ (μs) | $M_{0L}$ | $M_{0G}$ | $T_L$ (μs) | $T_G$ (μs) | $M_{0L}$ | $M_{0G}$ |
| *1* | 362.6 | 33.4 | 0.49 | 0.51 | 51.7 | 22.9 | 0.12 | 0.88 |
| *2* | 928.8 | 42.3 | 0.45 | 0.55 | 88.3 | 23.1 | 0.53 | 0.47 |
| *3* | 136.7 | 26.4 | 0.44 | 0.56 | 44.0 | 24.3 | 0.35 | 0.65 |
| *4* | 149.3 | 30.1 | 0.40 | 0.60 | 48.9 | 25.6 | 0.25 | 0.75 |
| *5* | 126.8 | 26.5 | 0.43 | 0.57 | 45.4 | 21.5 | 0.29 | 0.71 |
| *6* | 530.2 | 27.1 | 0.17 | 0.83 | 307.9 | 21.6 | 0.05 | 0.95 |

and account for about 51 – 83 % (Gaussian initial magnetization $M_{0G}$). Aromatic weakly coupled aromatic carbons with Lorentzian magnetization decay (nonprotonated carbons) have decay time constants $T_L$ that range from 127 to 929 µs and their fraction is between 17 – 49 % (Lorentzian initial magnetization $M_{0L}$).

The signal of nonprotonated aromatic carbons can be further decomposed into the three components. Signals of phenolic carbons are in the range of chemical shift $\delta$ from 150 to 165 ppm (aromatic ethereal carbons can be included). Alkylated aromatic carbons resonate at $\delta$ = 135 – 150 ppm. Signals of bridgehead carbons fall in the range of chemical shift lower than $\delta$ = 135 ppm. To determine the fraction of the above-mentioned carbons, the signal of aromatics was deconvoluted into three components. One component, which is reflected by a shoulder at $\delta \sim$ 150 ppm reflected the phenolic carbons fraction $f_a^P$. The second component (shoulder at $\delta \sim$ 140 ppm) corresponded to the fraction of alkylated aromatic carbons $f_a^S$. Both these fractions $f_a^P$ and $f_a^S$ was directly determined by the decomposition of the aromatic signal. The fraction of bridgehead carbons $f_a^B$ was obtained by subtracting the fraction of phenolic and alkylated aromatic carbons from the fraction of nonprotonated aromatic carbons

$$f_a^B = f_a - f_a^P - f_a^S \tag{5}$$

Aliphatic/cyclanic signal with a chemical shift at $\delta$ = 50 – 10 ppm was decomposed into two main components according to magnetization behaviour during $^1$H-$^{13}$C dipolar-dephasing experiments similarly as in the case of an aromatic signal. At first, the Gaussian magnetization decay reflects strongly proton-coupled aliphatic/cyclanic carbons (CH and $CH_2$). Fraction of protonated aliphatic/cyclanic carbons $f_{al}^H$ is to be calculated by

$$f_{al}^H = f_{al} M_{0G} \tag{6}$$

where $f_{al}$ is a fraction of aliphatic/cyclanic carbons ($f_{al}$ = 1.00 - $f_a$). Magnetization decay of strongly coupled carbons was described by the Gaussian decay time constants ranging from 22 to 26 µs with a fraction of about 47 – 95 % (the Gaussian initial magnetization intensity, Table 4). The Lorentzian magnetization decay corresponds with weakly proton-coupled carbons such as methyl and/or quaternary carbons. Their fraction $f_{al}^N$ is calculated as

$$f_{al}^N = f_{al} M_{0L} \tag{7}$$

The Lorentzian decay time constants in this region varied from 44 to 308 µs with initial Lorentzian magnetization intensity of 5 – 53 % for weakly coupled aliphatic/cyclanic carbons.

A higher fraction of strongly coupled carbons (aliphatic/cyclanic as well as aromatic) was found practically in all samples. Aliphatic/cyclanic carbons attached to oxygen resonate at $\delta$ = 50 – 90 ppm, however, the fraction of such carbons could not be directly determined by decomposition of the aliphatic/cyclanic carbons signal because only a small shoulder in this region was observed. As it followed from the $^1$H-$^{13}$C dipolar-dephasing experiments, the two main signals at $\delta$ 29 ppm and 21 ppm exist in the region $\delta$= 10 – 50 ppm. These signals reflect differently dipolarcoupled carbons to protons in groups. A much faster decay of the signal at $\delta$ = 29 ppm then corresponds with strongly dipolar coupled carbons ($CH_2$ and CH) contrary to slower magnetization decay of weakly coupled aliphatic/cyclanic carbons with the signal at $\delta$= 21 ppm (mainly $CH_3$). Fraction of methyl carbons $f_{al}^M$ was then directly determined by decomposition of the signal. By subtraction from $f_{al}^N$, the fraction of quaternary carbons $f_{al}^Q$ was calculated.

**Table 5** Fractions of carbons (distribution of structural carbons)

| Sample No. | $f_a$ | $f_a^H$ | $f_a^N$ | $f_a^P$ | $f_a^S$ | $f_a^B$ | $f_{al}$ | $f_{al}^H$ | $f_{al}^N$ | $f_{al}^M$ | $f_{al}^Q$ |
|---|---|---|---|---|---|---|---|---|---|---|---|
| *1* | 0.48 | 0.25 | 0.23 | 0.04 | 0.12 | 0.07 | 0.52 | 0.46 | 0.06 | 0.06 | 0.00 |
| *2* | 0.61 | 0.34 | 0.27 | 0.03 | 0.04 | 0.20 | 0.39 | 0.18 | 0.21 | 0.14 | 0.07 |
| *3* | 0.64 | 0.34 | 0.30 | 0.07 | 0.09 | 0.14 | 0.36 | 0.23 | 0.13 | 0.13 | 0.00 |
| *4* | 0.63 | 0.38 | 0.25 | 0.03 | 0.15 | 0.07 | 0.37 | 0.27 | 0.10 | 0.10 | 0.00 |
| *5* | 0.65 | 0.37 | 0.28 | 0.04 | 0.11 | 0.13 | 0.35 | 0.25 | 0.10 | 0.10 | 0.00 |
| *6* | 0.61 | 0.51 | 0.10 | 0.04 | 0.02 | 0.04 | 0.39 | 0.37 | 0.02 | 0.02 | 0.00 |

$f_a$ – aromaticity; $f_a^H$ – fraction of protonated aromatic carbons; $f_a^N$ – fraction of nonprotonated aromatic carbons; $f_a^P$ – fraction of phenol aromatic carbons; $f_a^S$ – fraction of alkylated aromatic carbons; $f_a^B$ – fraction of bridgehead aromatic carbons; $f_{al}$ – fraction of aliphatic/cyclanic carbons; $f_{al}^H$ – fraction of protonated aliphatic/cyclanic carbons (CH, $CH_2$); $f_{al}^N$ – fraction of nonprotonated aliphatic/cyclanic carbons (C, $CH_3$); $f_{al}^M$ – fraction of $CH_3$ carbons; $f_{al}^Q$ – fraction of quaternary carbons.

## RESULTS AND DISCUSSION

All determined values of the above-mentioned fractions are summarized in Table 5.

As the amount of bridgehead carbons $f_a^B$ generally increases with the increasing aromaticity $f_a$, the mole fraction of aromatic bridgehead carbons calculated as $\chi_B = f_a^B/f_a$ can be used to estimate the size of the aromatic cluster (aromatic-cyclanic unit in coal macromolecular network) as the number of aromatic carbon atoms per cluster. The basic model of relationship of $\chi_B$ to the structure of polycondensed aromatic clusters was well defined and described (Solum, Pugmire and Grant, 1989). According to the equation

$$\chi_B = \frac{1-\tanh\left(\frac{C-C_0}{m}\right)}{2}\left(\frac{1}{2}-\frac{3}{C}\right)+\frac{1+\tanh\left(\frac{C-C_0}{m}\right)}{2}\left(1-\frac{\sqrt{6}}{\sqrt{C}}\right) \qquad (8)$$

where $C$ is the number of aromatic carbon atoms per aromatic cluster and $C_0$ and $m$ are adjustable parameters, one can determine the number of carbons $C$ in an aromatic cluster. The values of adjustable parameters were $C_0 = 19.57$ and $m = 4.15$. The number of attachments per cluster can be defined as

$$C_{att} = C\frac{f_a^S + f_a^P}{f_a} \qquad (9)$$

The calculated $C$-values, i.e. the numbers of aromatic carbons per aromatic-cyclanic cluster, $\chi_B$-values and the numbers of structural aromatic and aliphatic/cyclanic carbons per cluster $C_a^i$ and $C_{al}^i$, respectively, are listed in Table 6.

On the basis of all calculated structural parameters we proposed the representative structures of coal samples (Fig. 2). One should take into account that every sample represents a mixture of wide series of different aromatic-cyclanic clusters, and the distribution of these clusters determines resulting structural parameters obtained by $^{13}$C CP/MAS NMR experiments. Therefore, the calculated parameters are only average values. In the Fig. 2 then two or three model structures represent the structure of coal maceral fraction.

In the coal structure oxygen plays an important role. Because aryl alkyl ethers and diaryl ethers were identified and quantified by the DRIFTS-PLS method in the studied separates (Straka and Endrýsová, 1999), ethereal oxygen was included in presented structures. Distribution of oxygen among oxygen functionalities showed that of 51 – 55 % of total oxygen is in the ethers, 40 – 46 % in phenols and only 3 – 5 % in carbonyls.

As representative structures of bituminous coals from Upper Silesian Coal Basin are the clusters with mainly 3 – 4 aromatic rings, 1 – 2 OH groups and six-membered cyclanes or oxygen-containing heterocyclanes with quaternary carbons and methyls, representative structures in Fig. 2 prove that in the Dukla coal the clusters with mainly with 1 – 2 aromatic rings, 1 OH groups and five- or six-membered cyclanes with methyls and quaternary carbons exist in coal polymers as prevailing form of aromatic-cyclanic units.

Wide range of Lorentzian decay time constants for aromatic carbons (Table 4) reflects a huge variability of structure of clusters. This Lorentzian component indicates the strength of $^1$H – $^{13}$C dipolar coupling between indirectly coupled nuclei with a relatively large distance within one cluster as well as bet-

**Table 6** Numbers of carbons (types of structural carbons) per cluster

| No. | $\chi_B$ | $C$ | $C_a^H$ | $C_a^N$ | $C_a^P$ | $C_a^S$ | $C_a^B$ | $C_{att}$ | $C_{al}$ | $C_{al}^H$ | $C_{al}^N$ | $C_{al}^M$ | $C_{al}^Q$ |
|---|---|---|---|---|---|---|---|---|---|---|---|---|---|
| *1* | 0.15 | 8-9 | 4-5 | 4 | 1 | 2 | 1 | 3 | 9 | 8 | 1 | 1 | 0 |
| *2* | 0.33 | 16-17 | 9 | 8 | 1 | 1 | 6 | 2 | 10-11 | 5 | 5-6 | 3-4 | 2 |
| *3* | 0.22 | 10-11 | 5-6 | 5 | 1 | 1-2 | 2 | 2-3 | 5-6 | 3-4 | 2 | 2 | 0 |
| *4* | 0.11 | 7-8 | 4-5 | 3 | 0-1 | 2 | 1 | 2 | 4-5 | 3-4 | 1 | 1 | 0 |
| *5* | 0.20 | 10 | 6 | 4 | 0-1 | 1-2 | 2 | 2 | 5 | 4 | 1 | 1 | 0 |
| *6* | 0.07 | 7 | 6 | 1 | 0-1 | 0-1 | 0-1 | 1 | 4-5 | 4 | 0-1 | 0-1 | 0 |

$\chi_B$ - the mole fraction of aromatic bridgehead carbons. $C_a^i = (f_a^i/f_a)\,C$; $C_{al}^i = (f_{al}^i/f_{al})\,C_{al}$, where $C_{al}$ was calculated from $f_{al} = C_{al}/(C_{al} + C)$.
$C$ - number of aromatic carbons; $C_a^H$ – number of protonated aromatic carbons, $C_a^N$ – number of nonprotonated aromatic carbons; $C_a^P$ – number of phenol aromatic carbons; $C_a^S$ – number of alkylated aromatic carbons; $C_a^B$ – number of bridgehead aromatic carbons; $C_{att}$ – number of attachments; $C_{al}$ – number of aliphatic/cyclanic carbons; $C_{al}^H$ – number of protonated aliphatic/cyclanic carbons (CH, $CH_2$); $C_{al}^N$ – number of nonprotonated aliphatic/cyclanic carbons (C, $CH_3$); $C_{al}^M$ – number of $CH_3$ carbons; $C_{al}^Q$ – number of quaternary carbons; all per cluster.

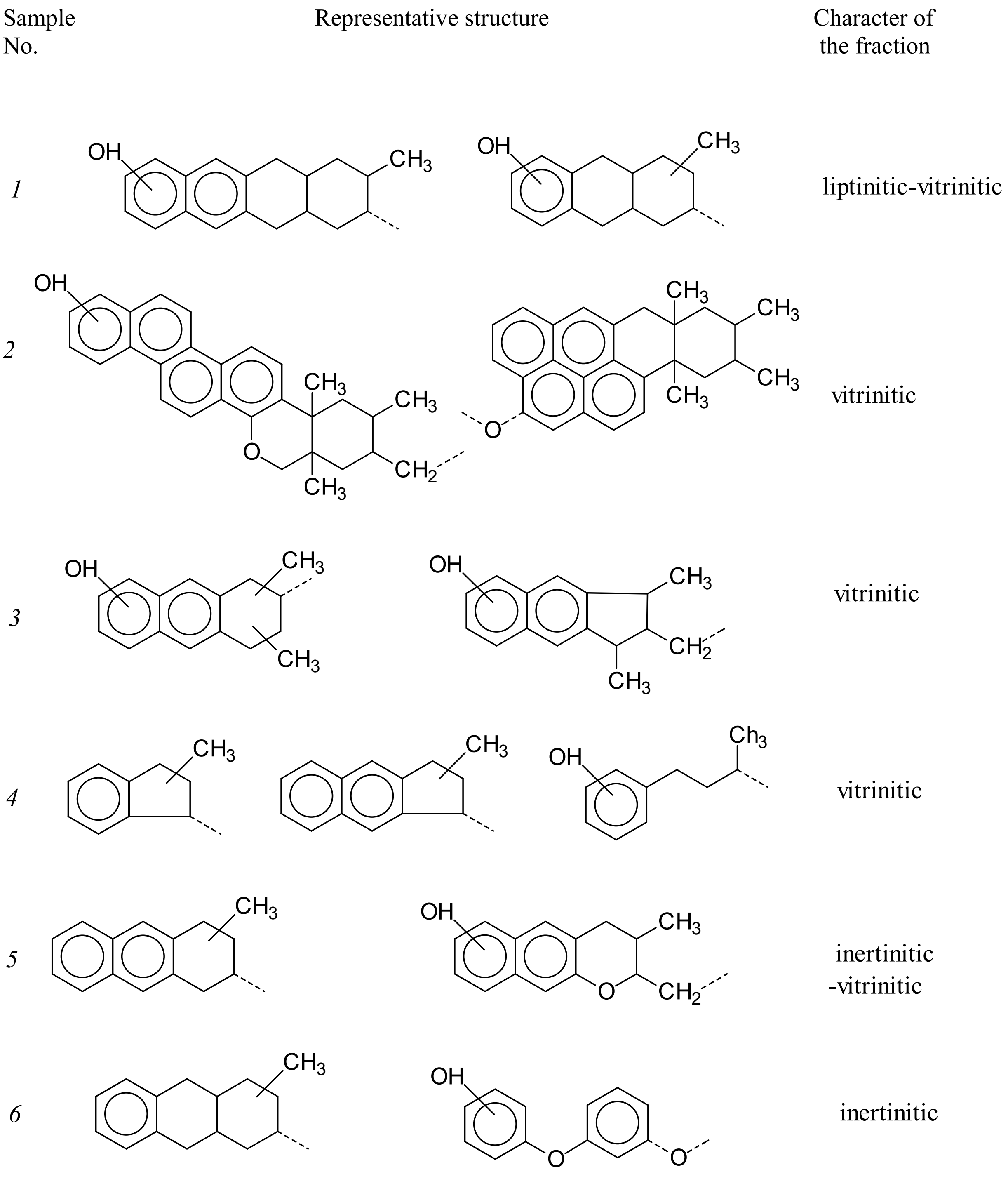

**Fig. 2** Representative structures of maceral fractions of the Dukla coal

ween neighbouring clusters. Therefore, the packing of clusters also determines this decay time constant. In addition, the dynamics of all clusters can affect this parameter. The shortest $T_L$ times (127, 137 and 149 μs) for the clusters in the samples *5*, *3* and *4*, respectively, indicate then compact packing of clusters and thus their low mobility, contrary to the samples *1*, *2* and *6* with the $T_L$ times of 363, 929 and 530 μs, respectively.

As Gaussian magnetization decay predominantly reflects the strength of dipolar interaction of directly coupled protons to carbons in aromatic rings, we observed a relatively narrow range of the Gaussian decay time constants. However, also in this case the shortest or shorter values $T_G$ correspond with the mobility of clusters and thus confirm their lower mobility and dense packing in the samples *3*, *4* and *5*, contrary to the samples *1* and *2*.

Similar characteristic features were also observed for dipolar dephasing decay time constants of aliphatic/cyclanic carbons. Small variation of Gaussian decay time constants (Table 4), which reflect dipolar interactions in CH and $CH_2$ groups, indicates that chains are short and form cyclanes. With longer and linear side chains one should expect wider variation in dynamic state and from this resulting wider range of Gaussian decay time constants, which should depend on a fraction of aliphatic/cyclanic carbons. Although the fraction of protonated aliphatic carbons ($f_{al}^{H}$ ) varies from 18 % to 46 % (Table 5), the $T_G$ times fall in the range from 22 μs to 26 μs (Table 4). High portion of cyclanes connected to aromatic rings is directly confirmed by the calculated numbers of attachments and CH and $CH_2$ groups per one aromatic-cyclanic cluster (Table 6).

As structures of maceral fractions *3*, *4* and *5* with a compact packing of clusters and their low mobility contain always only one five- or six-membered cyclanic ring, structures of maceral fractions *1*, *2* and *6* with higher mobility of clusters contain always two five- or six-membered cyclanic rings. It means that packing and mobility of clusters depends on a number of cyclanic rings.

Magnetization behaviour of the sample *6* with the lowest fraction of bridgehead aromatic carbons ($f_a^B$ = 0.04, Table 5) was different in comparison with the other ones. The magnetization decay of this sample was fast with low component of the Gaussian decay. The Gaussian decay time constant for aromatic carbons was low, but the Lorentzian decay time constant was high and the Gaussian initial magnetization of aromatic carbons was very high (Table 4). The same was observed for cyclanic carbons. Because the fraction of protonated aromatic carbons was very high in this case (51 %, Table 5), the proton density within the sample was also high. Because of very low amount of bridgehead aromatic carbons it can be deduced that simple aromatic rings exist in the sample in question. From high mobility of clusters and no compact packing of them (values $T_L$, Table 4) and high oxygen content, especially in ethereal oxygen (Table 7), it follows that the structure of the sample *6* is different in comparison with the other ones, as it is demonstrated in Fig. 2.

## ACKNOWLEDGEMENT

Grant Agency of Academy of Sciences of the Czech Republic supported this work as the grant project No. A2046902.

## REFERENCES

Solum, M. S., Pugmire, R. J.and Grant, D. M.: 1989, *Energy and Fuels* **3**, 187.

Straka, P. and Endrýsová, J.: 1999, *Chemical Papers* 53, 283.